Bisubstrate analog inhibitors of 6-hydroxymethyl-7,8-dihydropterin pyrophosphokinase: New lead exhibits a distinct binding mode

Genbin Shi [a], Gary Shaw [a], Yue Li [b], Yan Wu [b], Honggao Yan [b], Xinhua Ji [a,*]

[a] Macromolecular Crystallography Laboratory, National Cancer Institute, Frederick, MD 21702, USA
[b] Department of Biochemistry and Molecular Biology, Michigan State University, East Lansing, MI 48824, USA

ABSTRACT

6-Hydroxymethyl-7,8-dihydropterin pyrophosphokinase (HPPK), a key enzyme in the folate biosynthesis pathway catalyzing the pyrophosphoryl transfer from ATP to 6-hydroxymethyl-7,8-dihydropterin, is an attractive target for developing novel antimicrobial agents. Previously, we studied the mechanism of HPPK action, synthesized bisubstrate analog inhibitors by linking 6-hydroxymethylpterin to adenosine through phosphate groups, and developed a new generation of bisubstrate inhibitors by replacing the phosphate bridge with a piperidine-containing linkage. To further improve linker properties, we have synthesized a new compound, characterized its protein binding/inhibiting properties, and determined its structure in complex with HPPK. Surprisingly, this inhibitor exhibits a new binding mode in that the adenine base is flipped when compared to previously reported structures. Furthermore, the side chain of amino acid residue E77 is involved in protein–inhibitor interaction, forming hydrogen bonds with both 2′ and 3′ hydroxyl groups of the ribose moiety. Residue E77 is conserved among HPPK sequences, but interacts only indirectly with the bound MgATP via water molecules. Never observed before, the E77-ribose interaction is compatible only with the new inhibitor-binding mode. Therefore, this compound represents a new direction for further development.

Published by Elsevier Ltd.

1. Introduction

Folate cofactors are essential for all forms of life. With an active transport system, mammals obtain folates from their diet; lacking an active transport system, most microorganisms must synthesize folates de novo.[1] Hence, the folate biosynthesis pathway is one of the major targets for the development of antimicrobial agents.[2–6] For example, inhibitors of dihydropteroate synthase and dihydrofolate reductase, two enzymes in the pathway, are currently used in clinic as antibiotics.[7–9] 6-Hydroxymethyl-7,8-dihydropterin pyrophosphokinase (HPPK) is another enzyme in the folate pathway and is absent from mammals. Therefore, HPPK is an attractive target for developing novel antimicrobial agents; attempts have been made for decades.[10–15]

HPPK is currently the best understood pyrophosphokinase.[16,17] As shown in Figure 1A, HPPK catalyzes the transfer of pyrophosphate from ATP to 6-hydroxymethyl-7,8-dihydropterin (HP); the products of the reaction are AMP and 6-hydroxymethyl-7,8-dihy

dropterin pyrophosphate (HPPP).[18] The reaction follows an apparently ordered kinetic mechanism with MgATP binding to the enzyme first (K_d = 2.6–4.5 μM) followed by rapid addition of HP (K_d in the sub-μM range).[19–21] The catalytically competent active center is assembled only after both MgATP and HP are bound.[22,17]

We have been developing bisubstrate analog inhibitors of HPPK, among which P^1-(6-hydroxymethylpterin)-P^4-(5′-adenosyl)tetraphosphate (HP$_4$A, Fig. 1B)[14] and 5′-S-[1-(2-{[(2-amino-7,7-dimethyl-4-oxo-3,4,7,8-tetrahydropteridin-6-yl)carbonyl]amino}ethyl)piperidin-4-yl]-5′-thioadenosine (HP-18, Fig. 1C)[15] show promising enzyme binding and inhibition properties. The K_d value for the binding of HP$_4$A to HPPK is 0.47 μM with IC$_{50}$ = 0.44 μM.[14] The K_d value for the binding of HP-18 to HPPK is 2.55 μM with IC$_{50}$ = 3.16 μM.[14] As aforementioned, the K_d value for the binding of MgATP to HPPK is 2.6–4.5 μM. Therefore, both HP$_4$A and HP-18 are good inhibitors of the enzyme.

For optimized ligand binding, the adenine base and phosphate tail of ATP each forms four hydrogen bonds with HPPK, while HP forms six hydrogen bonds with the enzyme.[22,13,23] The crystal structures of HP$_4$A and HP-18 each in complex with HPPK [protein data bank (PDB) entry 1EX8 for HPPK·HP$_4$A and 3UDV for HPPK·HP-18] show that (1) the adenine base in each inhibitor forms four hydrogen bonds, (2) the phosphate bridge of HP$_4$A forms nine, whereas the linker in HP-18 forms three hydrogen bonds, and (3) the pterin moiety in HP$_4$A forms five, whereas the pterin moiety
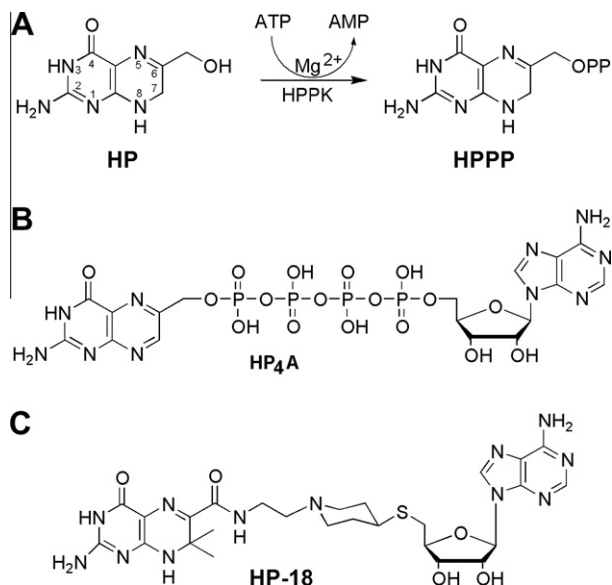
Figure 1. HPPK-catalyzed reaction and bisubstrate analog inhibitors of the enzyme. (A) The pyrophosphoryl transfer catalyzed by HPPK and chemical structures of the substrate and product of the reaction. (B) Chemical structure of bisubstrate analog inhibitor HP₄A.[14] (C) Chemical structure of bisubstrate analog inhibitor HP-18.[15]
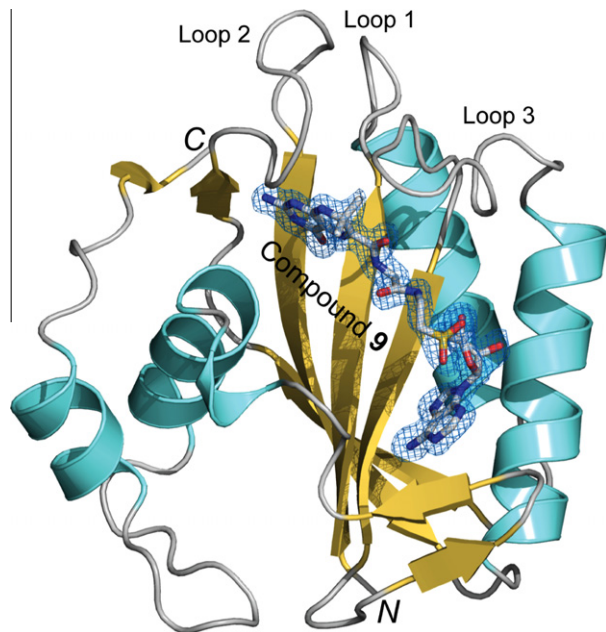

Figure 2. Schematic illustration of the HPPK·9 structure. Polypeptide chains are shown as a ribbon diagrams with helices (spirals) in cyan, strands (arrows) in orange, and loops (tubes) in grey. Compound 9 is shown as a stick model in atomic color scheme (C in grey, N in blue, O in red, and S in yellow) with electron density map ($2F_o$–F_c; contoured at 1.0 σ) as a blue net.

in HP-18 forms six hydrogen bonds with the enzyme.[14,15] Although HP-18 appears to bind to the enzyme not as tight as HP₄A does, it has two advantages. First, HP-18 optimizes the binding of both the pterin and adenine base moieties to the enzyme. Second, HP-18 has a linker that is more drug-like than the phosphate bridge that carries many negative charges and thereby leads to poor bioavailability. Furthermore, the structure of HPPK·HP-18 (PDB entry 3UDV) indicates that the oxidation of the sulfide in HP-18 to sulfone could enable the formation of more hydrogen bonds between

the linker of the inhibitor and the enzyme. Here, we report a new bisubstrate analog inhibitor of HPPK, which contains such a sulfone group but exhibits an unexpected binding mode when it is bound to HPPK. As an effort to maximize the interaction between the linker and the enzyme, the aminoethylpiperidine spacer in HP-18 (Fig. 1C) has been replaced with a glycyl aminoethyl spacer (Fig. 2) in the new compound.

2. Results and discussion

2.1. Synthesis

As illustrated in Scheme 1, under basic condition the sulfur nucleophile of (2-mercapto-ethyl)-carbamic acid *tert*-butyl ester (**2**) attacked 2′,3′-*O*-isopropylidene-5′-*O*-toluene-*p*-sulfonyl adeno sine (**1**) and gave compound 2-[6-(6-amino-purin-9-yl)-2,2-dimethyl-tetrahydro-furo[3,4-*d*][1,3]dioxol-4-ylmethylsulfanyl]-ethyl}-carbamic acid *tert*-butyl ester (**3**). The sulfide in **3** was then oxidized to the corresponding sulfone in {2-[6-(6-Amino-purin-9-yl)-2,2-dimethyl-tetrahydro-furo[3,4-*d*][1,3]dioxol-4-ylmethanesu lfonyl]-ethyl}-carbamic acid *tert*-butyl ester (**4**) using potassium hydrogen persulfate (oxone®) at 0 °C in methanol and sodium bicarbonate (pH 5). Under the TFA/DCM condition, cleavage of the BOC protection group yielded 9-[6-(2-Amino-ethanesulfonylmeth yl)-2,2-dimethyl-tetrahydro-furo[3,4-*d*][1,3]dioxol-4-yl]-9H-purin-6-ylamine (**5**). Amidation of **5** with Boc-glycine *N*-hydroxysuccini mide ester gave (2-{2-[6-(6-amino-purin-9-yl)-2,2-dimethyl-tetra hydro-furo[3,4-*d*][1,3]dioxol-4-ylmethanesulfonyl]-ethylcarbamoyl}-ethyl)-carbamic acid *tert*-butyl ester (**6**). Under the TFA/DCM condi tion, cleavage of the BOC protection group 1,3-dioxolanes gave compound 3-amino-*N*-{2-[5-(6-amino-purin-9-yl)-3,4-dihydroxy-tetrahydro-furan-2-ylmethanesulfonyl]-ethyl}-propionamide (**7**). Amidation of **7** with 2-amino-7,7-dimethyl-4-oxo-3,4,7,8-tetrahy dro-pteridine-6-carboxylic acid (**8**)[24,15] gave the final product 2-amino-7,7-dimethyl-4-oxo-3,4,7,8-tetrahydro-pteridine-6-carbox ylic acid (2-{2-[5-(6-amino-purin-9-yl)-3,4-dihydroxy-tetrahydro-furan-2-ylmethanesulfonyl]-ethylcarbamoyl}-ethyl)-amide (**9**).

2.2. HPPK binding and inhibition

The K_d and IC_{50} measurements were carried out as de-scribed[25,14] with sufficient details presented in the experimental methods (Section 4.2 and 4.3). The K_d value is 4.16 ± 0.25 μM, and the IC_{50} value is 9.53 ± 0.96 μM for compound **9**.

### 2.3. Crystal structure of compound 9 in complex with HPPK

The HPPK·**9** structure (Fig. 2) contains 1 HPPK (residues 1–158), 1 compound **9**, and 171 water molecules in the asymmetric unit. The statistics of X-ray diffraction data and structural refinement is summarized in Table 1.

2.4. Distinct binding mode of compound 9 to HPPK

2.4.1. Loop 3 of HPPK in the HPPK·9 structure is ordered

HPPK has three flexible loops (Loop 1, residues 8–15; Loop 2, residues 43–53; Loop 3, residues 82–92. Fig. 2), among which Loop 3 undergoes dramatic conformational changes during cataly-sis.[26,27] The catalytic trajectory of HPPK can be described by six consecutive states: apo-HPPK, HPPK·MgATP, HPPK·MgATP·HP, HPPK·MgAMP-PP-HP (the transition state), HPPK·AMP·HPPP, and HPPK·HPPP.[21,28] In the HPPK·MgATP·HP, HPPK·MgAMP-PP-HP, and HPPK·MgAMP·HPPP states, Loop 3 is closed.[28,22]

Although Loop 3 in the HPPK·HP-18 structure (PDB entry 3UDV) appears to assume the closed conformation, about 40% of the loop
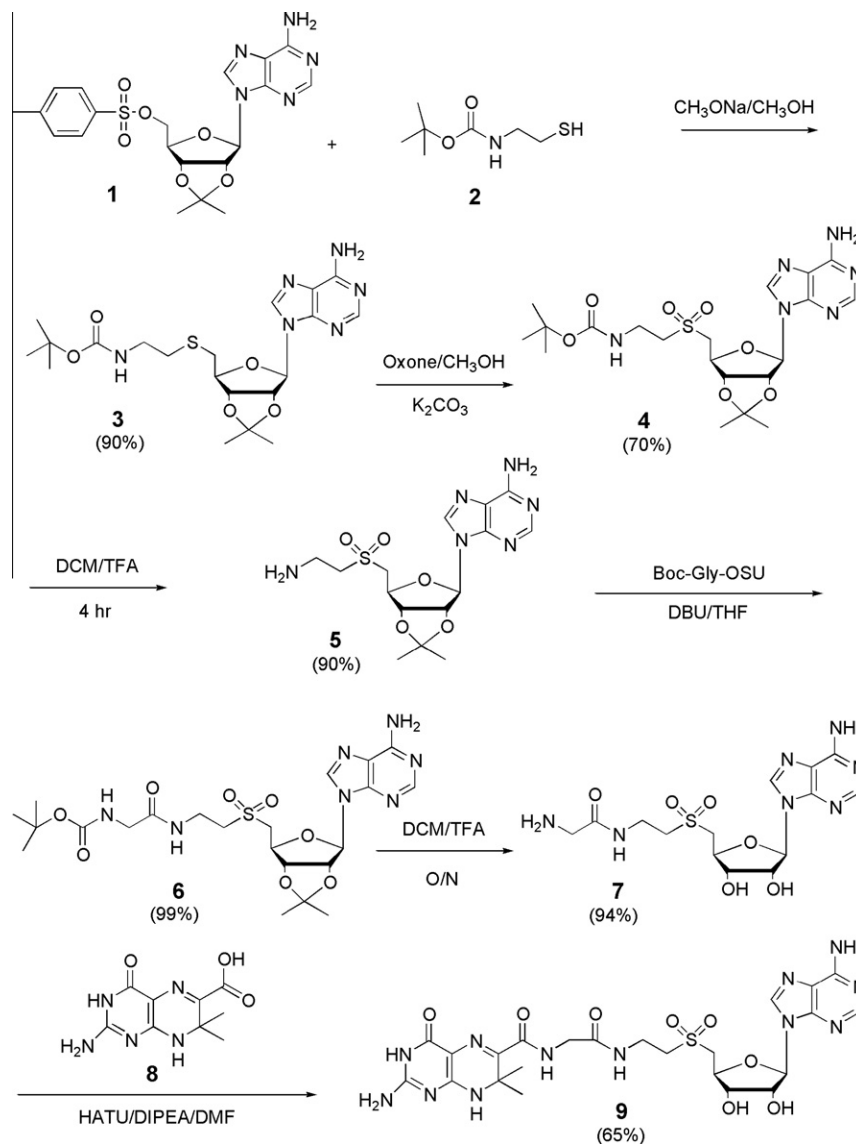
Scheme 1.

(residues 83–86) is disordered (Fig. 3A), which we believe is due to insufficient interaction between Loop 3 and the linker connecting the pterin and adenine moieties of the inhibitor.[15] In contrast, Loop 3 in the HPPK·9 structure, which assumes the closed conformation, is completely ordered (Figs. 2 and 3A).

The structure shows that a hydrogen bond is formed between the amino group of K85 and the ribose 2′ hydroxyl group of compound **9** (Fig. 3A). No other favored interactions are observed between Loop 3 and compound **9**. The HPPK·**9** structure shares the same crystal form with HPPK·HP-18 (PDB entry 3UDV) and the two structures superimpose very well with a root-mean-square deviation (RMSD) value of 0.133 Å for 518 out of 609 pairs of backbone atom (N, Cα, C, and O) positions. Therefore, it is this hydrogen bond between Loop 3 (side chain amino group of K85) and compound **9** (2′ hydroxyl group of ribose) that leads to the completely ordered Loop 3.

2.4.2. Adenine base of compound 9 is flipped

In the HPPK·HP-18 (PDB entry 3UDV) and HPPK·**9** structures, the interactions between the protein and the pterin moiety of inhibitors are identical (Fig. 3B and C). In contrast, the binding mode of the adenine base is distinct. The binding mode of the adenine base in HPPK·HP-18 is the catalytic binding model as observed in the catalytic center assembly of HPPK (PDB entry 1Q0N).[22] The adenine base in HPPK·**9** is, however, flipped with respect to the catalytic binding mode (Fig. 3A). Interestingly, the pattern of protein-adenine base interaction remains (Fig. 3B and C). In the superimposed HPPK·HP-18 and HPPK·**9** structures (Fig. 3A), the distance between the amino group of K85 (in HPPK·**9**) and the 2′ hydroxyl group of HP-18 (in HPPK·HP-18) is 6.1 Å, whereas the distance between the amino group of K85 (in HPPK·**9**) and the 2′ hydroxyl group of compound **9** (in HPPK·**9**) is 3.2 Å, indicating that the base flipping repositions the ribose moiety and thereby enables the formation of the hydrogen bond between Loop 3 and compound **9**. More importantly, such a gain in inhibitor binding is not at the expense of weakening protein-adenine base interaction.

2.4.3. Conserved E77 side chain is involved in the binding of compound 9

Residue E77 is conserved among HPPK sequences. In the catalytic center assembly (PDB entry 1Q0N), it interacts with Mg²⁺ via a water molecule and with α-phosphate via another water

Table 1
Crystal data, X-ray diffraction, and structure

Crystal	
Space group	$P2_12_12$
Unit cell parameters: a (Å)	53.12
b (Å)	70.58
c (Å)	36.26
Data	Overall (last shell)
Resolution (Å)	30.00–1.67 (1.73–1.67)
Unique reflections	14746 (802)
Redundancy	4.9 (2.5)
Completeness (%)	89.0 (49.1)
R_{merge}[a]	0.086 (0.411)
I/σ	15.3 (1.8)
Refinement	Overall (last shell)
Resolution (Å)	27.57–1.73 (1.82–1.73)
Unique reflections	13829 (1419)
Completeness (%)	93.6 (70.0)
Data in the test set	940 (97)
R-work	0.172 (0.277)
R-free	0.222 (0.349)
Structure	
Protein non-H atoms/B (Å^2)	1290 / 19.6
Ligand atoms/B (Å^2)	44 / 19.0
Water oxygen atoms/B (Å^2)	171 / 27.3
RMSD	
Bond lengths (Å)	0.012
Bond angles (°)	1.379
Coordinate error (Å)	0.51
Ramachandran plot[b]	
Favored regions (%)	96.8
Disallowed regions (%)	0.0

[a] $R_{merge} = \Sigma|(I-<I>)|/\Sigma(I)$, where I is the observed intensity.
[b] Obtained using Ramachandran data by Lovell et al.[36]

molecule.[22] In HPPK·HP-18 (PDB entry 3UDV), E77 has a van der Waals interaction (3.5 Å) with the inhibitor.[15] In the HPPK·9 complex, however, the E77 side chain forms two hydrogen bonds with the ribose (Fig. 3B), which is only possible for the repositioned ribose moiety. Taking into account the hydrogen bond between Loop 3 and ribose, the new binding mode of the adenosine moiety enhances the protein-adenosine interaction by two more hydrogen bonds than HP-18 (Fig. 3B and C).

2.4.4. The sulfone group of compound 9 is not in the position to interact with HPPK

The sulfone group of compound **9** is not positioned to interact with the protein due to the novel binding mode, but the structure suggests moderate modifications of compound **9** by moving the sulfone group away from the ribose may enhance protein-inhibitor interactions.

2.4.5. The new spacer in compound 9 does not form more hydrogen bonds with HPPK

As aforementioned, the aminoethylpiperidine spacer in HP-18 (Fig. 1C) was replaced with the glycyl aminoethyl spacer in compound **9** (Fig. 2). The new spacer forms only one hydrogen bond with HPPK (Fig. 3B), no better than the aminoethylpiperidine spacer (Fig. 3C). Nevertheless, the flexibility of the new spacer may be necessary for the new binding mode of the adenosine moiety of compound **9**.

3. Conclusions

We have been developing bisubstrate analog inhibitors for HPPK, which contains the pterin moiety, the adenine base moiety, and the linker connecting the two moieties. Here, we report a new lead molecule of such inhibitors, which was designed for improved

protein-linker interactions. As aforementioned, the K_d value for the binding of HP-18 to HPPK is 2.55 μM with an IC$_{50}$ value of 3.16 μM.[14] With a K_d value of 4.16 ± 0.25 μM and an IC$_{50}$ value of 9.53 ± 0.96 μM, compound **9** is not better than HP-18. Nevertheless, the new compound exhibits an unexpected, distinct binding mode to the protein. With respect to the catalytic binding mode, which has been observed in the catalytic center assembly, the new inhibitor (compound **9**) exhibits a flipped adenine base and repositioned ribose. This rearrangement enables the hydrogen bond formation between the hydroxyl groups of ribose with the side chains of E77 and K85. The K85-ribose interaction stabilizes Loop 3 and the E77-ribose interaction suggests how to use another conserved residue in the development of HPPK inhibitors. Compound **9**, therefore, represents a new lead for further improvement. Relocation of the sulfone group closer to the pterin moiety may results in protein-sulfone interactions that will certainly improve the affinity of bisubstrate analog inhibitors. To facilitate the sulfone relocation, the new glycyl aminoethyl spacer in compound **9** has certain advantage over the aminoethylpiperidine spacer in HP-18.

4. Experimental methods

4.1. Chemistry

4.1.1. General methods

All chemicals were purchased from Sigma–Aldrich except that compound **1** was purchased from TCI America. Starting materials and solvents were used without further purification. Anhydrous reactions were conducted under a positive pressure of dry N$_2$. Reactions were monitored by TLC, on Baker-flex Silica Gel IB-F (J. T. Baker). All compounds and intermediates were purified by flash chromatography performed on Teledyne ISCO Combiflash Rf system using RediSep Rf columns. Ion exchange chromatography was performed using strata Scx (50 μM particle size, 70 Å pore) resin cartridges. Preparative high pressure liquid chromatography (HPLC) was conducted using a Waters 600E system with a Waters 2487 dual λ absorbance detector and Phenomenex C$_{18}$ columns (250 mm × 21.2 mm, 5 μm particle size, 110 Å pore) at a flow rate of 10 mL/min. A binary solvent systems consisting of A = 0.1% aqueous TFA and B = 0.1% TFA in acetonitrile was employed with the gradients as indicated. ^{1}H and ^{13}C NMR data were obtained on a Varian 400 MHz spectrometer and are reported in ppm relative to TMS (tetramethylsilane). Mass spectra were measured with Agilent 1100 series LC/Mass Selective Detector, Agilent 1200 LC/MSD-SL system and Thermoquest Surveyor Finnigan LCQ deca. IR spectra were measured with a JASCO FT/IR 4100 spectrometer. Chemical purity was determined by HPLC analysis with a Zorbax Eclipse plus C18 column (Narrow Bore RR 2.1 mm × 50 mm, 3.5 micron; flow rate of 0.3 mL/min; solvent, methanol/H$_2$O gradient, 0.1% acetic acid; detection at 260 nm), confirming >95% purity.

4.1.2. 2-[6-(6-Amino-purin-9-yl)-2,2-dimethyl-tetrahydro-furo[3,4-d][1,3]dioxol-4-ylmethylsulfanyl]-ethyl}-carbamic acid tert-butyl ester (3)

A solution of compound **2** (1.77 g, 10.0 mmol) in NaOCH$_3$ (0.5 M in methanol, 20.2 mL, 10.1 mmol) was stirred under a nitrogen atmosphere for 15 min. Compound **1** (3.23 g, 7.0 mmol) was then added and the mixture was reflux for 5 h. After the reaction was finished, the solvent was removed under vacuum; the crude material was dissolved in ethyl acetate. The ethyl acetate solution was washed with saturated NaHCO$_3$, 5% HCl, and brine. The ethyl acetate solution was then dried with MgSO$_4$, filtered and evaporated to give the crude product. The title compound was obtained in 90% yield (2.94 g) after purification by flash chromatography. IR, ν_{max} (neat, cm^{-1}) 3332, 2980, 2934, 1696, 1640, 1598, 1366,
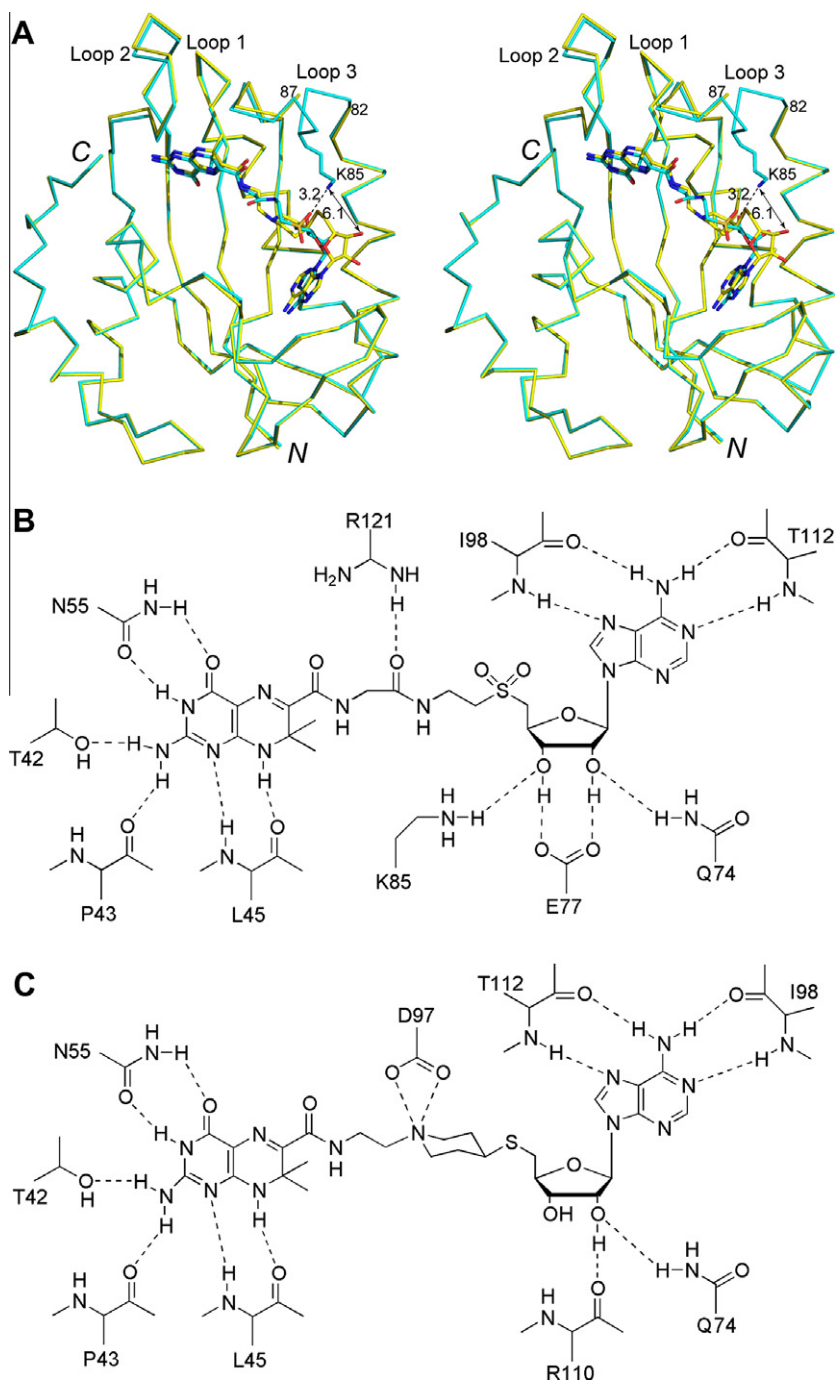
Figure 3. Structural comparison. (A) Stereoview showing the superimposed HPPK·**9** (in cyan, this work) and HPPK·HP-18 (in yellow, PDB entry 3UDV) structures. Proteins are shown as Cα traces and ligands as sticks. The side chain of K85 in the HPPK·**9** structure is also shown as a stick model. The dashed line indicates a hydrogen bond (3.2 Å) between the K85 amino group of HPPK and the ribose 2′ hydroxyl group of compound **9**. The double-headed arrow indicates a distance of 6.1 Å between the K85 amino group of HPPK and the ribose 2′ hydroxyl group of HP-18. (B) Protein–inhibitor interactions as observed in the HPPK·**9** structure. (C) Protein–inhibitor interactions as observed in the HPPK·HP-18 structure.

1248, 1208, 1161, 1086, 868. NMR δH (400 MHz; CD$_3$OD), 1.38 (3H, s), 1.41 (9H, s), 1.58 (3H, s), 2.60 (2H, t), 2.83 (2H, m), 3.17 (2H, m), 4.34 (1H, m), 5.06 (1H, m), 5.52 (1H, m), 6.18 (1H, d), 8.25 (1H, s), 8.28 (1H, s); δ^{13}C (100 MHz; CD$_3$OD), 158.03 (1C), 157.23 (1C), 153.95 (1C), 150.08 (1C), 141.66 (1C), 120.48 (1C), 115.36 (1C), 91.52 (1C), 87.73 (1C), 85.06 (1C), 84.93 (1C), 79.97 (1C), 41.08 (1C), 34.90 (1C), 33.03 (1C), 28.74 (3C), 27.39 (1C), 25.55 (1C); HRMS (ESI-MS) calcd for C$_{20}$H$_{30}$N$_6$O$_5$S (MH$^+$): 467.2071; found: 467.2082.

4.1.3. {2-[6-(6-Amino-purin-9-yl)-2,2-dimethyl-tetrahydro-furo[3,4-*d*][1,3]dioxol-4-ylmethanesulfonyl]-ethyl}-carbamic acid *tert*-butyl ester (4)

Potassium carbonate powder (0.28 g, 2.0 mmol) was carefully added to a solution of potassium hydrogen persulfate (1.84 g, 3.0 mmol), water (15 mL), until the final pH of the aqueous solution was 5. The oxone solution was added dropwise to a solution of compound **3** (0.47 g 1.0 mmol) in methanol (15 mL) which was cooled to 0 °C while stirring, and the reaction mixture was

stirred at room temperature overnight. The solution was extracted three times between ethyl acetate and water, and the organic layer was dried over MgSO₄. The organic layer was concentrated and the title compound was obtained in 70% yield (0.35 g) after purification by flash chromatography. IR, v_{max} (neat, cm⁻¹) 3345, 2979, 2921, 1694, 1651, 1236, 1165, 1090, 1022, 894, 871. NMR δH (400 MHz; CD₃OD), 1.37 (12H, s), 1.59 (3H, s), 3.09–3.21 (2H, m), 3.27–3.39 (2H, m), 3.61 (1H, q), 3.82 (1H, q), 4.71 (1H, m), 5.23 (1H, q), 5.47 (1H, q), 6.26 (1H, d), 8.25 (1H, s), 8.27 (1H, s); δ¹³C (100 MHz; CD₃OD), 157.66 (1C), 157.30 (1C), 154.04 (1C), 149.86 (1C), 142.14 (1C), 120.71 (1C), 115.78 (1C), 90.90 (1C), 85.26 (1C), 85.06 (1C), 82.91 (1C), 80.41 (1C), 57.12 (1C), 54.69 (1C), 34.82 (1C), 28.68 (3C), 27.40 (1C), 25.56 (1C); HRMS (ESI-MS) calcd for $C_{20}H_{30}N_6O_7S$ (MH⁺): 499.1969; found: 499.1976.

4.1.4. 2-Amino-7,7-dimethyl-4-oxo-3,4,7,8-tetrahydro-pteridine-6-carboxylic acid (2-{2-[5-(6-amino-purin-9-yl)-3,4-dihydroxy-tetrahydro-furan-2-ylmethanesulfonyl]-ethylcarbamoyl}-ethyl)-amide (9)

To a solution of compound **4** (0.50 g, 1.0 mmol) in 5 mL DCM, 1 mL TFA was added dropwise at −20 °C; then the reaction mixture was stirred at room temperature for a few hours. After the reaction was finished, the solvent was removed under vacuum, and the residue was purified by silica gel chromatography, eluting with 15% DCM/methanol, to afford 0.36 g (90%) of the compound **5** as white foam. A solution of Boc-L-Gly-OSu (0.27 g, 1.0 mmol) in dry THF (10 mL) was treated with the product, and the resulting suspension was cooled at 0 °C under nitrogen. A solution of DIPEA (0.2 mL, 1.1 mmol) in dry THF (4.0 mL) was added. Stirring was continued overnight, and then the solvent was evaporated. The crude product was dissolved in ethyl acetate and purified by flash chromatography. The product, compound **6** (0.5 g, 99%), was dissolved in 5 mL DCM, and 2 mL TFA was added dropwise at −20 °C. Then, the reaction mixture was stirred at room temperature overnight. After the reaction was finished, the solvent was removed under vacuum, and the residue was purified by silica gel chromatography, eluting with 15% DCM/methanol, to afford 0.35 g (94%) of compound **7**. The product was added to a solution of compound **8** (0.20 g, 0.84 mmol), O-(7-azabenzotriazol-1-yl)-1,1,3,3-tetramethyluronium hexafluorophosphate (HATU) (0.33 g, 0.88 mmol), and DIPEA (411 μl, 2.4 mmol)) in anhydrous DMF (50 mL). After 18 h at room temperature, the solvent was evaporated under high vacuum, and the reaction residue was purified by HPLC (H₂O/Methanol) to give the final product, compound **9** (0.35 g, 0.55 mmol, 65%). IR, v_{max} (neat, cm⁻¹) 3101, 2796, 2360, 1655, 1508, 1432, 1292, 1196, 1130, 834, 798, 721. NMR δH (400 MHz; CD₃OD), 1.57 (6H, s), 3.23–2.28 (2H, m), 3.30–3.33 (1H, m), 3.43–3.52 (3H, m) 3.54–3.88 (3H, m), 4..43–4.45 (1H,t), 4.49–4.53 (1H, m), 6.07 (1H, d,), 8.45 (1H, s), 8.48 (1H, s); δ¹³C (100 MHz; DMSO-d₆), 169.15 (1C), 163.72 (1C), 158.84 (1C), 155.39 (1C), 149.03 (1C), 143.80 (1C), 142.48 (1C), 119.67 (1C), 117.78 (1C), 114.86(1C), 110.00 (1C), 100.80 (1C), 88.62 (1C), 79.36 (1C), 73.37 (1C), 72.93 (1C), 56.38 (1C), 53.97 (1C), 53.18 (1C), 42.04 (1C), 32.58 (1C), 28.49 (2C); HRMS (ESI-MS) calcd for $C_{23}H_{30}N_{12}O_8S$ (MH⁺): 635.2103; found: 635.2116.

4.2. Fluorometric titration

The dissociation constants of the inhibitors were measured as described[25] for the fluorometric measurement of the dissociation constant of Ant-ATP with modifications. Briefly, the inhibitors were dissolved in dimethylsulfoxide. Dimethylsulfoxide concentrations were kept within 1.7% during the titration experiments and control experiments showed that dimethylsulfoxide at these concentrations had no effects on activity (substrate binding and catalysis) of the enzyme. Escherichia coli HPPK was dissolved in 100 mM Tris,
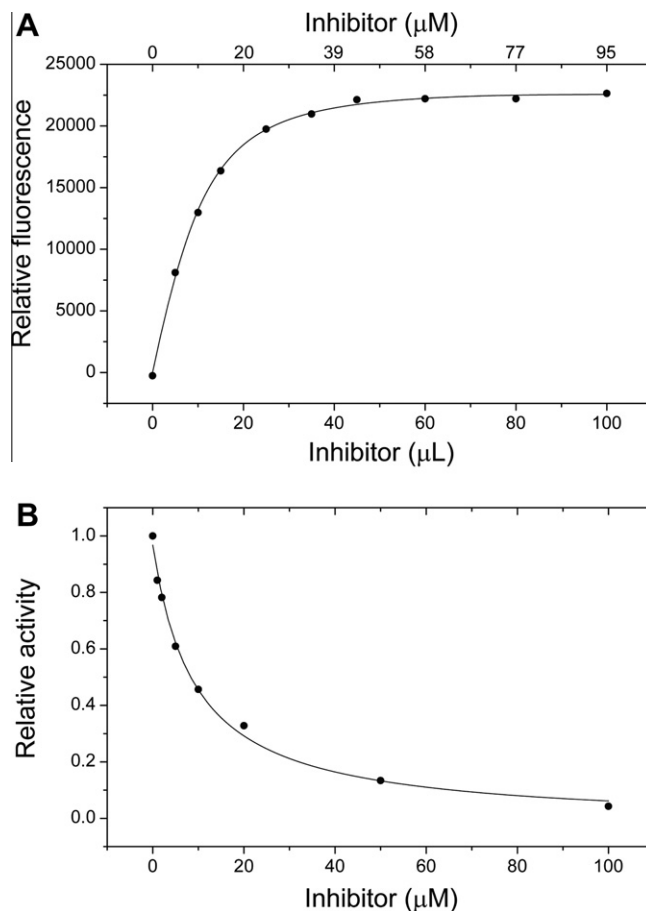

Figure 4. K_d and IC₅₀ measurements. (A) Fluorometric titration of HPPK with compound **9**. (B) Inhibition of HPPK by compound **9**.

pH 8.3. The titration was performed at 23 °C by adding aliquots of a 2 mM compound **9** stock solution to the HPPK solution. The initial HPPK concentration and volume were 10 μM and 2 mL, respectively. The excitation and emission wavelengths were 450 and 480 nm, respectively. The excitation and emission slits were 1 and 4 nm, respectively. The K_d values were obtained by nonlinear least-squares regression of the data to Eq. (1) as described[25]

$$\Delta F_{obs} = \frac{\Delta F_{mol}(K_d + E_t + L_t - \sqrt{(K_d + E_t + L_t)^2 - 4E_tL_t})}{2} \quad (1)$$

where ΔF_{obs} and ΔF_{mol} are observed and molar fluorescence changes caused by binding, E_t is the total concentration of HPPK, and L_t is the total concentration of the inhibitor. As an example, the fluorometric titration of HPPK with compound **9** is shown in Figure 4A.

4.3. Enzyme inhibition assay

IC₅₀ measurements were carried out essentially as described.[14] Briefly, the initial reaction mixtures in 30 μl contained 1 nM E. coli HPPK, 2 μM ATP, 1 μM HP, 5 mM MgCl₂, 25 mM DTT, and a trace amount of [α-³²P]-ATP (∼1 μCi) in 100 mM Tris, pH 8.3. The experiments were conducted at 23 °C. The reaction was initiated by the addition of the enzyme and stopped 30 min later by the addition of 6 μl of 0.5 M EDTA. The radioactive reactant and product were separated by thin-layer chromatography, using a PEI-cellulose plastic plate (EMD) with 0.3 M KH₂PO₄ as the mobile phase, and quantified by a Phosphor-Imager system (Amersham Typhoon 9200). The IC₅₀ values were obtained by fitting the data to a logistic

equation by nonlinear least-squares regression of the data to Eq. (2) as described[29]

$$v = v_{min} + \frac{v_{max} - v_{min}}{1 + \frac{[I]}{IC_{50}}} \qquad (2)$$

where v is the reaction rate, v_{min} the minimum reaction rate, v_{max} the maximum reaction rate, and [I] the concentration of the inhibitor. The inhibition of HPPK by compound **9** is shown in Figure 4B.

4.4. Crystallization, X-ray diffraction, structure solution, and refinement

A Hydra II-Plus-One crystallization robot (Matrix Technologies, Hudson, New Hampshire, USA) and Crystal Screen kits from Hampton Research (Laguna Niguel, California, USA) were used. Crystals of HPPK·**9** were grown at 19 ± 1 °C in sitting drops containing 0.3 µl protein solution (10 mg/mL HPPK with saturated compound **9** in 20 mM Tris–HCl pH 8.0) and 0.3 µl well solution (25% PEG-3350 and 0.2 M NaCl in 0.1 M HEPES, pH 7.5). A crystal of HPPK·**9** was soaked in a cryoprotectant solution containing 75% (v/v) well solution and 25% (v/v) ethylene glycol, and flash-cooled in liquid nitrogen. X-ray diffraction data were collected at 100 K with an MARCCD detector mounted at the synchrotron Beamline 22 at the Advanced Photon Source, Argonne National Laboratory. Data processing was carried out with the HKL2000 program suite.[30] The structure was solved by Fourier synthesis starting with the HPPK·HP-18 structure (PDB entry 3UDV).[15] Multiple conformations of amino acid residues, ligands, and solvent molecules were removed from the starting model. Structure solution and refinement were done with PHENIX.[31] All graphics work, including model building and rebuilding, was performed with COOT.[32] The structures were verified with annealed omit maps and the geometry was assessed using PROCHECK[33] and WHAT IF.[34] The statistics of X-ray diffraction data and the HPPK·**9** structure are summarized in Table 1. Illustrations were prepared with PyMOL.[35]

Acknowledgments

The coordinates and structure factors for the HPPK·**9** complex have been deposited in the PDB under entry code 4F7V.

Supplementary data

Supplementary data associated with this article can be found, in the online version, at http://dx.doi.org/10.1016/j.bmc.2012.05.060.

References and notes

1. Hitchings, G. H.; Burchall, J. J. *Adv. Enzymol. Relat. Areas Mol. Biol.* **1965**, *27*, 417.
2. Cohen, M. L. *Science* **1992**, *257*, 1050.
3. Neu, H. C. *Science* **1992**, *257*, 1064.
4. Murray, B. E. *Adv. Intern. Med.* **1997**, *42*, 339.
5. Bermingham, A.; Derrick, J. P. *Bioessays* **2002**, *24*, 637.
6. Walsh, C. *Nat. Rev. Microbiol.* **2003**, *1*, 65.
7. Hughes, D. T. D. *Sulphonamides. Antibiotic and Chemotherapy*, 7th ed.; Churchill Livingstone: New York, 1997.
8. Hughes, D. T. D. In *Antibiotics and Chemotherapy*; O'Grady, F., Lambert, H. P., Finch, R. G., Greenwood, D., Eds.; Churchill Livingstone: New York, 1997; pp 346–356.
9. Zinner, S. H.; Mayer, K. H. In *Principles and Practice of Infectious Diseases*; Mandell, G. L., Bennett, J. E., Dolin, R., Eds.; Churchill Livingstone: Philadelphia, 2005; pp 440–451.
10. Wood, H. C. S. In *Chemistry and Biology of Pteridines*; Pfleiderer, W., Ed.; Walter de Gruyter: Berlin–New York, 1975.
11. Al-Hassan, S. S.; Cameron, R. J.; Curran, A. W. C.; Lyall, W. J. S.; Nicholson, S. H.; Robinson, D. R.; Stuart, A.; Suckling, C. J.; Stirling, I.; Wood, H. C. S. *J. Chem. Soc., Perkin Trans. 1* **1985**, 1645.
12. Hennig, M.; Dale, G. E.; D'Arcy, A.; Danel, F.; Fischer, S.; Gray, C. P.; Jolidon, S.; Muller, F.; Page, M. G.; Pattison, P.; Oefner, C. *J. Mol. Biol.* **1999**, *287*, 211.
13. Stammers, D. K.; Achari, A.; Somers, D. O.; Bryant, P. K.; Rosemond, J.; Scott, D. L.; Champness, J. N. *FEBS Lett.* **1999**, *456*, 49.
14. Shi, G.; Blaszczyk, J.; Ji, X.; Yan, H. *J. Med. Chem.* **2001**, *44*, 1364.
15. Shi, G.; Shaw, G.; Liang, Y. H.; Subburaman, P.; Li, Y.; Wu, Y.; Yan, H.; Ji, X. *Bioorg. Med. Chem.* **2012**, *20*, 47.
16. Derrick, J. P. In *Folic Acid and Folates*; Litwack, G., Ed.; Academic Press: Oxford, UK, 2008; pp 411–433.
17. Yan, H.; Ji, X. *Protein Pept. Lett.* **2011**, *18*, 328.
18. Shiota, T. In *Chemistry and Biochemistry of Folates*; Blakley, R. T., Benkovic, S. J., Eds.; John Wiley & Sons: New York, 1984; pp 121–134.
19. Shi, G.; Gong, Y.; Savchenko, A.; Zeikus, J. G.; Xiao, B.; Ji, X.; Yan, H. *Biochim. Biophys. Acta* **2000**, *1478*, 289.
20. Bermingham, A.; Bottomley, J. R.; Primrose, W. U.; Derrick, J. P. *J. Biol. Chem.* **2000**, *275*, 17962.
21. Li, Y.; Gong, Y.; Shi, G.; Blaszczyk, J.; Ji, X.; Yan, H. *Biochemistry* **2002**, *41*, 8777.
22. Blaszczyk, J.; Shi, G.; Yan, H.; Ji, X. *Structure* **2000**, *8*, 1049.
23. Blaszczyk, J.; Li, Y.; Shi, G.; Yan, H.; Ji, X. *Biochemistry* **2003**, *42*, 1573.
24. Shi, G.; Ji, X. *Tetrahedron Lett.* **2011**, *52*, 6174.
25. Li, Y.; Wu, Y.; Blaszczyk, J.; Ji, X.; Yan, H. *Biochemistry* **2003**, *42*, 1581.
26. Xiao, B.; Shi, G.; Chen, X.; Yan, H.; Ji, X. *Structure* **1999**, *7*, 489.
27. Xiao, B.; Shi, G.; Gao, J.; Blaszczyk, J.; Liu, Q.; Ji, X.; Yan, H. *J. Biol. Chem.* **2001**, *276*, 40274.
28. Blaszczyk, J.; Shi, G.; Li, Y.; Yan, H.; Ji, X. *Structure (Camb)* **2004**, *12*, 467.
29. Graeser, D.; Neubig, R. R. In *Signal Transduction*; Milligan, G., Ed.; IRL Press: Oxford, 1992; pp 1–30.
30. Otwinowski, Z.; Minor, W. *Methods Enzymol.* **1997**, *276*, 307.
31. Adams, P. D.; Grosse-Kunstleve, R. W.; Hung, L. W.; Ioerger, T. R.; McCoy, A. J.; Moriarty, N. W.; Read, R. J.; Sacchettini, J. C.; Sauter, N. K.; Terwilliger, T. C. *Acta Crystallogr., Sect. D* **2002**, *58*, 1948.
32. Emsley, P.; Cowtan, K. *Acta Crystallogr., Sect. D* **2004**, *60*, 2126.
33. Laskowski, R. A.; MacArthur, M. W.; Moss, D. S.; Thornton, J. M. *J. Appl. Crystallogr.* **1993**, *26*, 283.
34. Vriend, G. *J. Mol. Graphics Modell.* **1990**, *8*, 29.
35. *The PyMOL Molecular Graphics System*; DeLano, W. L., Ed.; Delano Scientific: San Carlos, CA, 2002.
36. Lovell, S. C.; Davis, I. W.; Arendall, W. B., 3rd; de Bakker, P. I.; Word, J. M.; Prisant, M. G.; Richardson, J. S.; Richardson, D. C. *Proteins: Struct. Funct. Genet.* **2003**, *50*, 437.